GEOLOGY | THE GEOLOGICAL SOCIETY OF AMERICA®

https://doi.org/10.1130/G46571.1

Manuscript received 28 May 2019
Revised manuscript received 19 July 2019
Manuscript accepted 6 August 2019

Published online 30 August 2019

Linking the progressive expansion of reducing conditions to a stepwise mass extinction event in the late Silurian oceans

Chelsie N. Bowman[1], Seth A. Young[1], Dimitri Kaljo[2], Mats E. Eriksson[3], Theodore R. Them II[4], Olle Hints[2], Tõnu Martma[2] and Jeremy D. Owens[1]

[1]Department of Earth, Ocean and Atmospheric Science–National High Magnetic Field Laboratory, Florida State University, Tallahassee, Florida 32306, USA

[2]Department of Geology, Tallinn University of Technology, Ehitajate tee 5, 19086 Tallinn, Estonia

[3]Department of Geology, Lund University, Sölvegatan 12, SE-223 62 Lund, Sweden

[4]Department of Geology and Environmental Geosciences, College of Charleston, Charleston, South Carolina 29424, USA

ABSTRACT

The late Ludlow Lau Event was a severe biotic crisis in the Silurian, characterized by resurgent microbial facies and faunal turnover rates otherwise only documented during the "big five" mass extinctions. This asynchronous late Silurian marine extinction event preceded an associated positive carbon isotope excursion (CIE), the Lau CIE, although a mechanism for this temporal offset remains poorly constrained. Here, we report thallium isotope data from locally reducing late Ludlow strata within the Baltic Basin to document the earliest onset of global marine deoxygenation. The initial expansion of anoxia coincided with the onset of the extinction and therefore preceded the Lau CIE. Additionally, sulfur isotope data record a large positive excursion parallel to the Lau CIE, interpreted to indicate an increase in pyrite burial associated with the widely documented CIE. This suggests a possible global expansion of euxinia (anoxic and sulfidic water column) following deoxygenation. These data are the most direct proxy evidence of paleoredox conditions linking the known extinction to the Lau CIE through the progressive expansion of anoxia, and most likely euxinia, across portions of the late Silurian oceans.

INTRODUCTION

High rates of evolutionary turnover and severe, punctuated extinctions of marine taxa were hallmarks of the Silurian (e.g., Jeppsson, 1998; Crampton et al., 2016). These events occurred during the transition from the Late Ordovician icehouse to Devonian greenhouse worlds, when a dynamic ocean-atmosphere system oscillated between cool and warm conditions (e.g., Jeppsson, 1998). Recurrent extinctions in graptolites and conodonts were associated with the transitions between the alternating climate states, the most notable being the globally documented late Ludlow Lau extinction (Jeppsson, 1998; Calner, 2005; Crampton et al., 2016). This extinction was first recognized using conodonts from carbonate platform successions (termed the Lau Event; e.g., Jeppsson and Aldridge, 2000) and then in graptolite studies of deeper-water shale successions (termed the Kozlowskii event; Koren', 1993; Urbanek, 1993), herein referred to as the Lau/Kozlowskii extinction (LKE). The LKE is at least the tenth largest extinction event in Earth history, with ~23% loss of genera (e.g., Bond and Grasby, 2017, and references therein). In addition to conodonts and graptolites, it affected a wide range of marine taxa, including brachiopods (Talent et al., 1993), fishes (Eriksson et al., 2009), and acritarchs (Stricanne et al., 2006). Extinctions of individual taxonomic groups were asynchronous, with documented extinctions in benthic and nektonic groups preceding the planktic organisms (e.g., Munnecke et al., 2003; Stricanne et al., 2006; Calner, 2008). The LKE shares similar characteristics to the "big five" mass extinctions, such as the survival of disaster fauna and a resurgence of microbially mediated sedimentary facies (e.g., Talent et al., 1993; Jeppsson, 2005; Calner, 2005, 2008; Eriksson et al., 2009).

Despite the magnitude and complexity of the LKE, its mechanistic underpinnings are not well constrained. An expansion of reducing conditions has been implicated as a potential driver of the observed stepwise extinction (e.g., Munnecke et al., 2003; Stricanne et al., 2006). This hypothesis is also used to explain the possibility of extensive burial of organic carbon, resulting in the Lau positive carbon isotope excursion (CIE; e.g., Saltzman, 2005), but this cannot explain the temporal offset between the LKE and the Lau CIE. Further, organic carbon burial can be affected by other factors (e.g., Canfield, 1994). Variations in eustatic sea level and carbonate weathering rates have also been invoked as potential mechanisms for driving positive CIEs (e.g., Hirnantian CIE; Kump et al., 1999). A global expansion of reducing conditions, however, provides a kill mechanism and can be tested using combined traditional and novel paleoredox proxies.

This study investigated the relationship between the LKE and Lau CIE in the context of changing marine redox conditions in Upper Silurian (Ludfordian Stage) strata from the Baltic Basin. In order to reconstruct the evolution of global marine redox conditions, we measured thallium (Tl) isotopes, manganese (Mn) concentrations, and pyrite sulfur isotopes ($\delta^{34}S_{pyr}$) from a distal shelf/slope setting (Latvia), and

CITATION: Bowman, C.N., et al., 2019, Linking the progressive expansion of reducing conditions to a stepwise mass extinction event in the late Silurian oceans: Geology, v. 47, p. 968–972, https://doi.org/10.1130/G46571.1

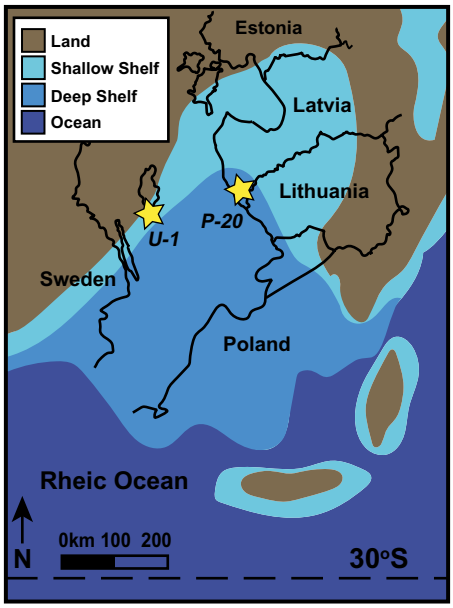

Figure 1. Paleogeographic reconstruction of the late Silurian Baltic Basin region (modified from the Blakey Europe Series, Silurian ca. 425 Ma; https://www2.nau.edu/rcb7/). Locations of Gotland (Sweden) localities and the Latvian Priekule-20 drill core are marked by yellow stars. Detailed discussion of correlation and biostratigraphy of our two localities can be found in the Data Repository (see footnote 1).

carbonate-associated sulfate (CAS) sulfur isotopes ($\delta^{34}S_{CAS}$) from a shallow shelf setting (Gotland, Sweden; Fig. 1). This multiproxy, multilithology approach aimed to establish first-order links among the fossil record of stepwise extinction, carbon burial, and the progression from more oxygenated to more reducing conditions in the late Silurian seas.

GEOLOGIC SETTING

In the late Silurian, the Baltic Basin was located in a tropical, epicratonic seaway on the southern margin of the paleocontinent Baltica (e.g., Eriksson and Calner, 2008; Fig. 1; Fig. DR1 in the GSA Data Repository[1]). The northern and eastern edges of the basin were delineated by rimmed carbonate shelves with parallel facies belts ranging from lagoonal deposits in the north to deep shelf shales and marls in the south, deepening toward the Rheic Ocean (Eriksson and Calner, 2008). The Uddvide-1 drill core and nearby outcrops on the island of Gotland, Sweden, are predominantly composed of carbonates from the shallow shelf area of the basin (for more details, see Eriksson and Calner, 2008). The Priekule-20 drill core from southwestern Latvia predominantly consists of shales and marls from a correlative deep shelf setting (details in Kaljo et al., 1997).

METHODS AND RESULTS

Two study localities were analyzed for $\delta^{13}C$ records, organic or inorganic (micrite), to investigate carbon cycle dynamics. Pyrite sulfur was extracted from shale samples using a widely accepted chromium reduction method, and CAS was extracted from carbonates following standard methods. Full details of all analytical methods are given in the Data Repository. Sulfur isotopes were analyzed to investigate global pyrite burial ($\delta^{34}S_{CAS}$) and the potential imprints on local signatures ($\delta^{34}S_{pyr}$). Sedimentary Tl isotopes ($\varepsilon^{205}Tl = [\{R_{sample}/R_{reference}\} - 1] \times 10^4$) have been used to investigate the earliest onset of global marine deoxygenation during Mesozoic CIEs (Ostrander et al., 2017; Them et al., 2018). During Mn-oxide precipitation, Tl is adsorbed with a large positive isotope fractionation, thus leaving seawater isotopically lighter (as reviewed in Nielsen et al., 2017). Precipitation and burial of Mn-oxides require oxic bottom-water conditions, the expanse of which represents the dominant seawater control of Tl isotope composition on time scales <~5 m.y. (Nielsen et al., 2017; Owens et al., 2017). The global seawater Tl isotope signal is recorded in euxinic marine settings and in anoxic waters with sulfide near the sediment-water interface from basins that are well connected to the open ocean (Owens et al., 2017). Consequently, reconstruction of the Tl isotope composition of late Silurian seawater provides evidence for initial changes in global marine oxygenation by tracking the burial flux of Mn-oxides relative to the extinction, CIE, and additional redox proxies (e.g., Ostrander et al., 2017; Them et al., 2018). Importantly, a large Tl isotope fractionation is not associated with the burial of other Mn-bearing minerals (e.g., sulfides, carbonates). Constraints on locally reducing conditions using an independent geochemical proxy are necessary to interpret Tl isotopes as a temporal seawater signature and to avoid contamination via local Mn-oxides (Owens et al., 2017). Low total Mn concentrations [Mn] are indicative of locally reducing conditions (e.g., Boyer et al., 2011) and thus were utilized in this study.

The Lau CIE is documented in the $\delta^{13}C_{carb}$ and $\delta^{13}C_{org}$ records from the outer shelf setting (Fig. 2A), with values increasing within the upper part of the graptolite *Bohemograptus*

[1]GSA Data Repository item 2019342, analytical methods, geochemical data, and cross plots, is available online at http://www.geosociety.org/datarepository/2019/, or on request from editing@geosociety.org.

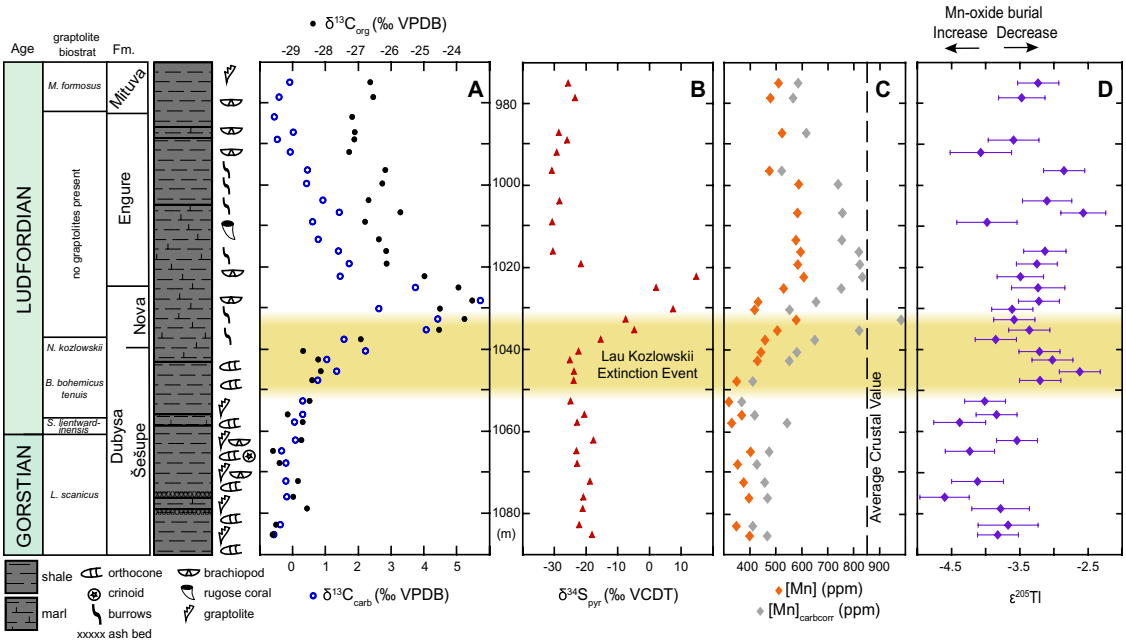

Figure 2. Geochemical data from the Priekule-20 drill core, near Priekule, Latvia. Graptolite biozones are after Kaljo et al. (1997). Lau/Kozlowskii extinction interval is shaded in yellow. *L.*—*Lobograptus*; *S.*—*Saetograptus*; *B.*—*Bohemograptus*; *N.*—*Neocucullograptus*; *M.*—*Monograptus*. (A) Carbonate and organic carbon isotope data. VPDB—Vienna Peedee belemnite. (B) Pyrite sulfur isotope data. VCDT—Vienna Canyon Diablo troilite. (C) Manganese concentration data, with dashed line representing average crustal values. (D) Thallium isotope data plotted with 2σ error bars.

bohemicus tenuis–Neocucullograptus kozlowskii zones, reaching peak values of + 5.7‰ and −23.5‰, respectively, in the Nova Beds of the Dubysa Formation. The $\delta^{13}C$ records return to baseline values in the overlying Engure Formation. There is a positive ~40‰ excursion in $\delta^{34}S_{pyr}$ data (baseline values ~−22‰ shift to peak values of up to ~+15‰) that coincides with the Lau CIE within the upper Nova Beds and basal Engure Formation (Fig. 2B). [Mn] values are low throughout the section, with average values of 363 and 552 ppm in the lower to middle Dubysa and Engure Formations, respectively (Fig. 2C). The $\varepsilon^{205}Tl$ record shows baseline values in the lower to middle Dubysa section of −4.1 to −4.6 (Fig. 2D). This is followed by a positive excursion in $\varepsilon^{205}Tl$ values that peaks at −2.6 and averages −3.3 throughout the rest of the drill core.

The Lau CIE is also documented in both the $\delta^{13}C_{carb}$ and $\delta^{13}C_{org}$ records from the inner shelf carbonates (Fig. 3A), with values beginning to rise in the upper När Formation and peaking in the overlying Eke Formation (conodont *Icriodontid* Zone) at +7.5‰ and −24.0‰, respectively. Within the Burgsvik Sandstone, $\delta^{13}C_{carb}$ values decline to ~+4.0‰, while $\delta^{13}C_{org}$ values increase to −22.9‰, which is followed by a return to peak $\delta^{13}C_{carb}$ values of +7.5‰ in the overlying Burgsvik Oolite (conodont *Ozarkodina snajdri* Zone). The overlying Hamra and Sundre Formations record the falling limb of the CIE, but not post-excursion baseline values. There is a positive ~30‰ excursion in the $\delta^{34}S_{CAS}$ record (Fig. 3B), with initial values ~+11‰ in the När Formation that rise through the Eke Formation to values of ~+22‰. The $\delta^{34}S_{CAS}$ values then continue rising through the Burgsvik Oolite, Hamra, and Sundre Formations to +40.6‰.

DISCUSSION

The [Mn] values from the Latvia deep shelf setting (Fig. 2C) are all below the average crustal values and suggest depleted local Mn deposition, and therefore locally reducing conditions throughout the studied interval (Boyer et al., 2011). A cross-plot of [Mn] and Tl isotopes shows no significant correlation (Fig. DR2I). Thus, it is unlikely that local Mn-oxide burial influenced the Tl isotope seawater signature. The observed positive shift in $\varepsilon^{205}Tl$ from ~−4.6 to − 2.6 begins within the Ludfordian *B. bohemicus tenuis* graptolite biozone (Fig. 2D) and signifies a decline in the global burial of Mn-oxides. The reduction in Mn-oxide burial was likely due to significant bottom-water deoxygenation as anaerobic microbial metabolisms kept pace with carbon export, reducing bottom-water oxidants such as oxygen and Mn-oxides, but not yet reducing them enough to increase widespread organic carbon preservation and burial (e.g., Ostrander et al., 2017; Them et al., 2018). This early onset of deoxygenation coincided with the initial phase of extinction (e.g., brachiopods, fish, and conodonts) that predated the Lau CIE (Fig. 4; e.g., Calner, 2008). Extinctions in these nektonic and benthic taxa coincide with the rising limb of the positive Tl isotope excursion, which begins ~8 m before the Lau CIE. This suggests that deoxygenation and the subsequent spread of anoxia were responsible for the initial phases of extinction in faunas living at or near the sediment-water interface and within deeper waters ~175–270 k.y. prior to the Lau CIE (see the Data Repository for calculations). For the first time in the Paleozoic, this stratigraphic relationship between extinction/turnover and carbon isotopes and Tl isotopes is observed. A similar progression of events has been suggested for two Mesozoic oceanic anoxic events (OAEs; Ostrander et al., 2017; Them et al., 2018), but with varying magnitudes and durations.

The positive carbon and sulfur isotope excursions (Figs. 2 and 3) are consistent with transient increases in the amount of reduced carbon and sulfur buried globally as organic matter, pyrite, and possibly organic sulfur compounds (e.g., Gill et al., 2011; Owens et al., 2013; Raven et al., 2019). Sea level may also have been a contributing, but secondary, factor to the Lau CIE (see the Data Repository for further discussion). This suggests that the Lau CIE began as export and burial of organic carbon to the seafloor outpaced consumption via remineralization, which was likely dependent on a sufficiently large portion of shelf and other marine environments being affected by deoxygenation and expansion of anoxia. The excess organic matter available fueled microbial sulfate reduction (MSR) and ultimately increased pyrite burial as MSR-produced H_2S reacted with reactive iron minerals in sulfidic environments. The burial fractions of reduced carbon and sulfur were preferentially enriched in ^{12}C and ^{32}S due to fractionation associated with biological processes, and the remaining seawater was enriched in ^{13}C and ^{34}S. Euxinic conditions possibly expanded into a greater portion of the oceans at the onset of the Lau CIE, as denoted by positive excursions in $\delta^{34}S_{pyr}$ and $\delta^{34}S_{CAS}$ (Figs. 2B and 3B). This onset of euxinia temporally coincided with the second wave of extinctions that affected planktic groups (i.e., ~75% loss in biodiversity of graptolites) and the rising limb of the CIE (Fig. 4A). Phytoplankton (e.g., acritarchs) actually increased in abundance immediately prior to and during the rising limb of the Lau CIE (Stricanne et al., 2006) as reducing conditions expanded, likely due to a lack of predation as zooplankton and larger marine taxa experienced

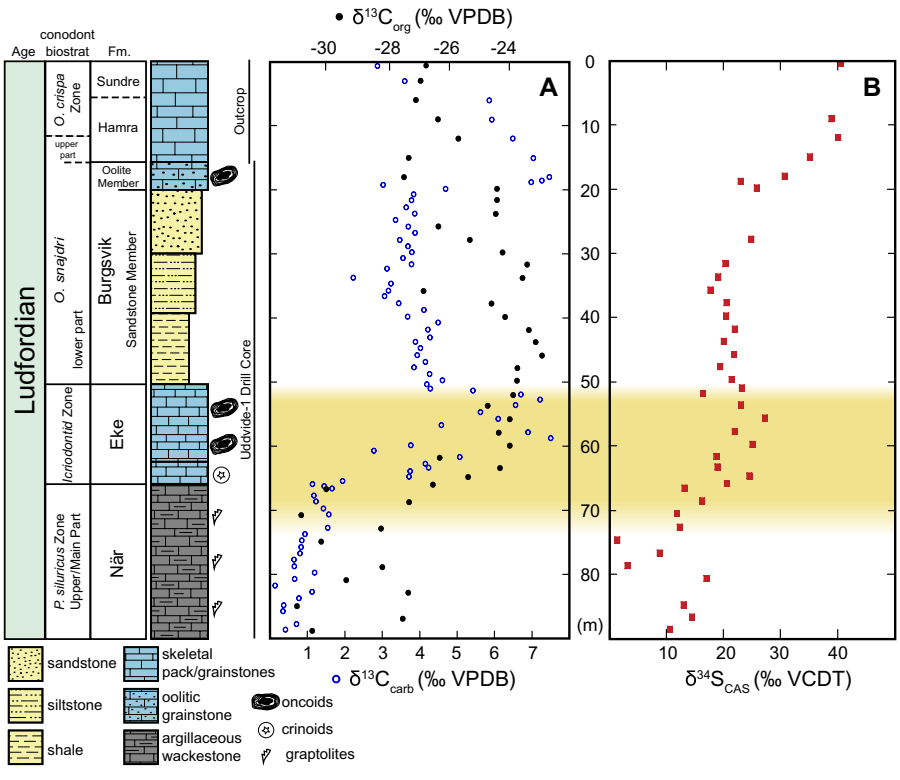

Figure 3. Geochemical data from the Uddvide-1 drill core and nearby outcrops on Gotland, Sweden. Conodont biozones are after Jeppsson (2005). Lau/Kozlowskii extinction interval is shaded in yellow. *P.*—*Polygnathoides*; *O.*—*Ozarkodina*. (A) Carbonate and organic carbon isotope data. VPDB—Vienna Peedee belemnite. (B) Carbonate-associated sulfate (CAS) sulfur isotope data. VCDT—Vienna Canyon Diablo troilite.

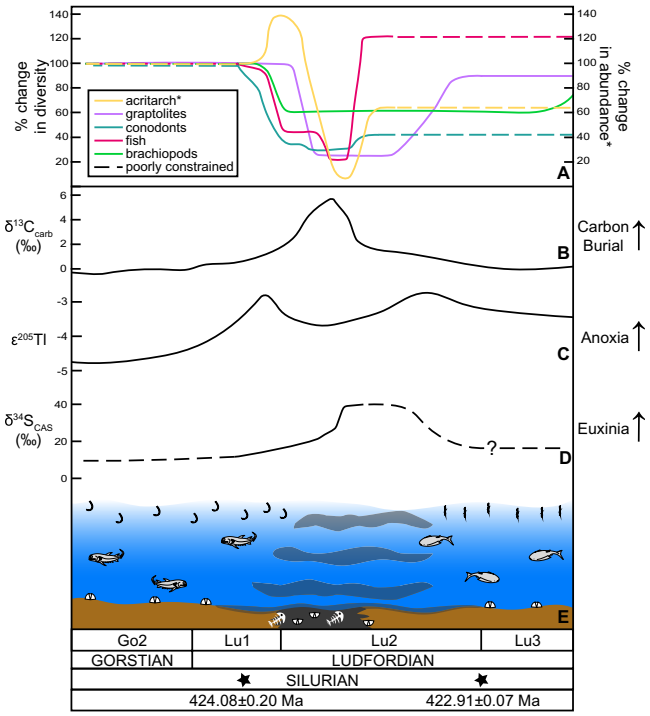

Figure 4. Summary of biotic, geochemical, and oceanographic events in the late Silurian that culminated in the Lau/Kozlowskii extinction (LKE) and Lau carbon isotope excursion (CIE). (A) Biotic data for acritarch (Stricanne et al., 2006), graptolite (Manda et al., 2012), conodont (Calner, 2008), fish (Eriksson et al., 2009), and brachiopod (Talent et al., 1993) extinctions. (B) Carbonate carbon isotope record. (C) Thallium isotope record indicating increased oceanic anoxia. (D) Carbonate-associated sulfate (CAS) sulfur isotope record suggesting increased euxinia; dashed portions are expected, but currently unconstrained trends. (E) Depiction of the biotic and marine redox changes throughout the Gorstian and Ludfordian. Stars mark positions of U-Pb zircon dates on K-bentonite ash beds from Podolia, Ukraine (Cramer et al., 2015). Construction of this figure is detailed in the Data Repository (see footnote 1).

earlier extinctions. Acritarchs finally declined with an associated ~95% drop in abundance during the peak of the CIE just before the global extent of euxinia reached a maximum, which is inferred by the rising limb nearing the peak of the $\delta^{34}S_{CAS}$ values.

In both the Gotland and Latvia $\delta^{34}S$ records, peak excursion values postdate the corresponding peak $\delta^{13}C$ values in the Lau CIE. The offset in these records suggests that organic carbon burial fueled high MSR rates, but it may also be related to differences in oceanic residence times and/or continued pyrite burial post-CIE (e.g., Owens et al., 2013). The falling limb of the $\delta^{34}S_{pyr}$ record also lags the falling limb of the CIE, perhaps indicating the continued consumption of previously exported organic carbon after the termination of the burial event, which is corroborated by Tl isotopes not returning to baseline values (cf., Them et al., 2018). Regardless of the C-S offset and isotopic magnitudes, these large-magnitude S-isotope excursions that span ~1 m.y. require a reduction in the marine sulfate reservoir, which was likely significantly lower than modern seawater (e.g., Gill et al., 2011).

CONCLUSIONS

The integrated paleontological and geochemical records suggest a stepwise extinction for the LKE that was associated with the progressive expansion of reducing marine conditions. Increased anoxic and euxinic conditions likely shoaled from deeper shelf/slope areas to shallow platform settings during the Lau CIE. Our Tl isotope data provide detailed evidence for expanding marine deoxygenation in the interval that preceded the Lau CIE, coinciding with the initial phase of extinction. This was followed by global carbon and sulfur isotope perturbations that coincided with continued marine extinction. This study highlights the role of oxygen depletion (i.e., nonsulfidic anoxia) near the onset of biotic change and provides a mechanism for the previously documented stepwise extinction event. The progressive expansion of oceanic anoxia leading to euxinia is a potential mechanism for extinction due to significant stress on marine ecosystems (Meyer and Kump, 2008), which might be similar to at least two Mesozoic OAEs. More broadly, this study indicates that global marine redox dynamics were a major driver in the evolution of the late Silurian biosphere, and potentially other Paleozoic biotic crises. The multiproxy redox approach provides a more holistic global view of redox changes and supports recent evidence suggesting prevalent low-oxygen conditions in the upper oceans of the Paleozoic (Lu et al., 2018).

ACKNOWLEDGMENTS

We thank N. Kozik, C. Richbourg, S. Newby, and E. Benayoun for assistance in sample processing and data collection; M. Calner for access to the Uddvide-1 core; four anonymous reviewers for their helpful reviews; and Judith Parrish for editorial handling of this manuscript. This research was funded by the National Science Foundation (grant EAR-1748635 to Young and Owens) and the Estonian Research Council (grant PUT611 to Kaljo, Hints, and Martma). This work was performed at the National High Magnetic Field Laboratory (Tallahassee, Florida), which is supported by National Science Foundation Cooperative Agreement No. DMR-1644779 and the State of Florida.

REFERENCES CITED

Bond, D.P.G., and Grasby, S.E., 2017, On the causes of mass extinctions: Palaeogeography, Palaeoclimatology, Palaeoecology, v. 478, p. 3–29, https://doi.org/10.1016/j.palaeo.2016.11.005.

Boyer, D.L., Owens, J.D., Lyons, T.W., and Droser, M.L., 2011, Joining forces: Combined biological and geochemical high-resolution palaeooxygen history in Devonian epeiric seas: Palaeogeography, Palaeoclimatology, Palaeoecology, v. 306, p. 134–146, https://doi.org/10.1016/j.palaeo.2011.04.012.

Calner, M., 2005, A Late Silurian extinction event and anachronistic period: Geology, v. 33, p. 305–308, https://doi.org/10.1130/G21185.1.

Calner, M., 2008, Silurian global events—At the tipping point of climate change, *in* Elewa, A.M.T., ed., Mass Extinctions: Berlin, Springer-Verlag, p. 21–57, https://doi.org/10.1007/978-3-540-75916-4_4.

Canfield, D.E., 1994, Factors influencing organic carbon preservation in marine sediments: Chemical Geology, v. 114, p. 315–329, https://doi.org/10.1016/0009-2541(94)90061-2.

Cramer, B.D., Schmitz, M.D., Huff, W.D., and Bergström, S.M., 2015, High-precision U-Pb zircon age constraints on the duration of rapid biogeochemical events during the Ludlow Epoch (Silurian Period): Journal of the Geological Society [London], v. 172, p. 157–160, https://doi.org/10.1144/jgs2014-094.

Crampton, J.S., Cooper, R.A., Sadler, P.M., and Foote, M., 2016, Greenhouse-icehouse transition in the Late Ordovician marks a step change in extinction regime in the marine plankton: Proceedings of the National Academy of Sciences of the United States of America, v. 113, p. 1498–1503, https://doi.org/10.1073/pnas.1519092113.

Eriksson, M.E., Nilsson, E.K., and Jeppsson, L., 2009, Vertebrate extinctions and reorganizations during the Late Silurian Lau event: Geology, v. 37, p. 739–742, https://doi.org/10.1130/G25709A.1.

Eriksson, M.J., and Calner, M., 2008, A sequence stratigraphical model for the late Ludfordian (Silurian) of Gotland, Sweden: Implications for timing between changes in sea level, palaeoecology, and the global carbon cycle: Facies, v. 54, p. 253–276, https://doi.org/10.1007/s10347-007-0128-y.

Gill, B.C., Lyons, T.W., Young, S.A., Kump, L.R., Knoll, A.H., and Saltzman, M.R., 2011, Geochemical evidence for widespread euxinia in the later Cambrian ocean: Nature, v. 469, p. 80–83, https://doi.org/10.1038/nature09700.

Jeppsson, L., 1998, Silurian oceanic events: Summary of general characteristics, *in* Landing, E., and Johnson, M.E., eds., Silurian Cycles: Linkages of Dynamic Stratigraphy with Atmospheric, Oceanic, and Tectonic Changes: James Hall Centennial Volume: Albany, New York, New York State Museum Bulletin 491, p. 239–257.

Jeppsson, L., 2005, Conodont-based revisions of the late Ludfordian on Gotland, Sweden: Geologiska Föreningen, v. 127, p. 273–282, https://doi.org/10.1080/11035890501274273.

Jeppsson, L., and Aldridge, R.J., 2000, Ludlow (Late Silurian) oceanic episodes and events: Journal of the Geological Society [London], v. 157, p. 1137–1148, https://doi.org/10.1144/jgs.157.6.1137.

Kaljo, D., Kiipli, T., and Martma, T., 1997, Carbon isotope event markers through the Wenlock-Pridoli sequence at Ohesaare (Estonia) and Priekule (Latvia): Palaeogeography, Palaeoclimatology, Palaeoecology, v. 132, p. 211–223, https://doi.org/10.1016/S0031-0182(97)00065-5.

Koren, T.N., 1993, Main event levels in the evolution of the Ludlow graptolites: Geological Correlation, v. 1, p. 44–52.

Kump, L.R., Arthur, M.A., Patzowsky, M.E., Gibbs, M.T., Pinkus, D.S., and Sheehan, P.M., 1999, A weathering hypothesis for glaciation at high atmospheric pCO_2 during the Late Ordovician: Palaeogeography, Palaeoclimatology, Palaeoecology, v. 152, p. 173–187, https://doi.org/10.1016/S0031-0182(99)00046-2.

Lu, W., et al., 2018, Late inception of a resiliently oxygenated upper ocean: Science, v. 361, p. 174–177, https://doi.org/10.1126/science.aar5372.

Manda, S., Štorch, P., Slavík, L., Fryda, J., Kríž, J., and Tasáryová, A., 2012, The graptolite, conodont and sedimentary record through the late Ludlow Kozlowskii event (Silurian) in the shale-dominated succession of Bohemia: Geological Magazine, v. 149, no. 3, p. 507–531, https://doi.org/10.1017/S0016756811000847.

Meyer, K.M., and Kump, L.R., 2008, Oceanic euxinia in Earth history: Causes and consequences: Annual Reviews of Earth and Planetary Science Letters, v. 36, p. 251–288, https://doi.org/10.1146/annurev.earth.36.031207.124256.

Munnecke, A., Samtleben, C., and Bickert, T., 2003, The Ireviken event in the Lower Silurian of Gotland, Sweden—Relation to similar Palaeozoic and Proterozoic events: Palaeogeography, Palaeoclimatology, Palaeoecology, v. 195, p. 99–124, https://doi.org/10.1016/S0031-0182(03)00304-3.

Nielsen, S.G., Rehkämper, M., and Pritulak, J., 2017, Investigation and application of thallium isotope fractionation: Reviews in Mineralogy and Geochemistry, v. 82, p. 759–798, https://doi.org/10.2138/rmg.2017.82.18.

Ostrander, C.M., Owens, J.D., and Nielsen, S.G., 2017, Constraining the rate of oceanic deoxygenation leading up to a Cretaceous oceanic anoxic event (OAE-2: ~94 Ma): Science Advances, v. 3, p. e1701020, https://doi.org/10.1126/sciadv.1701020.

Owens, J.D., Gill, B.C., Jenkyns, H.C., Bates, S.M., Severmann, S., Kuypers, M.M.M., Woodfine, R.G., and Lyons, T.W., 2013, Sulfur isotopes track the global extent and dynamics of euxinia during Cretaceous oceanic anoxic event 2: Proceedings of the National Academy of Sciences of the United States of America, v. 110, p. 18407–18412, https://doi.org/10.1073/pnas.1305304110.

Owens, J.D., Nielsen, S.G., Horner, T.J., Ostrander, C.M., and Peterson, L.C., 2017, Thallium-isotope compositions of euxinic sediments as a proxy for global manganese-oxide burial: Geochimica et Cosmochimica Acta, v. 213, p. 291–307, https://doi.org/10.1016/j.gca.2017.06.041.

Raven, M.R., Fike, D.A., Bradley, A.S., Gomes, M.L., Owens, J.D., and Webb, S.A., 2019, Paired organic matter and pyrite $\delta^{34}S$ records reveal mechanisms of carbon, sulfur, and iron cycle disruption during ocean anoxic event 2: Earth and Planetary Science Letters, v. 512, p. 27–38, https://doi.org/10.1016/j.epsl.2019.01.048.

Saltzman, M.R., 2005, Phosphorus, nitrogen, and the redox evolution of the Paleozoic oceans: Geology, v. 33, p. 573–576, https://doi.org/10.1130/G21535.1.

Stricanne, L., Munnecke, A., and Pross, J., 2006, Assessing mechanisms of environmental change: Palynological signals across the late Ludlow (Silurian) positive isotope excursion ($\delta^{13}C$, $\delta^{18}O$) on Gotland, Sweden: Palaeogeography, Palaeoclimatology, Palaeoecology, v. 230, p. 1–31, https://doi.org/10.1016/j.palaeo.2005.07.003.

Talent, J.A., Mawson, R., Andrew, A.S., Hamilton, P.J., and Whitford, D.J., 1993, Middle Paleozoic extinction events: Faunal and isotopic data: Palaeogeography, Palaeoclimatology, Palaeoecology, v. 104, p. 139–152, https://doi.org/10.1016/0031-0182(93)90126-4.

Them, T.R., II, Gill, B.C., Caruthers, A.H., Gerhardt, A.M., Gröcke, D.R., Lyons, T.W., Marroquin, S.M., Nielsen, S.G., Trabucho Alexandre, J.P., and Owens, J.D., 2018, Thallium isotopes reveal protracted anoxia during the Toarcian (Early Jurassic) associated with volcanism, carbon burial, and mass extinction: Proceedings of the National Academy of Sciences of the United States of America, v. 115, p. 1–6, https://doi.org/10.1073/pnas.1803478115.

Urbanek, A., 1993, Biotic crises in the history of the Upper Silurian graptoloids: A paleobiological model: Historical Biology, v. 7, p. 29–50, https://doi.org/10.1080/10292389309380442.

Printed in USA